PROCEEDINGS OF SPIE

SPIEDigitalLibrary.org/conference-proceedings-of-spie

Design of Al-free and Al-based InGaAs/GaAs strained quantum well 980-nm pump lasers including thermal behavior effects on E/O characteristics

Sergio Pellegrino, M. G. Re, C. Beoni, D. Reichenbach, F. Vidimari

Sergio Pellegrino, M. G. Re, C. Beoni, D. Reichenbach, F. Vidimari, "Design of Al-free and Al-based InGaAs/GaAs strained quantum well 980-nm pump lasers including thermal behavior effects on E/O characteristics," Proc. SPIE 2150, Design, Simulation, and Fabrication of Optoelectronic Devices and Circuits, (2 May 1994); doi: 10.1117/12.175004

SPIE.

Event: OE/LASE '94, 1994, Los Angeles, CA, United States

Downloaded From: https://www.spiedigitallibrary.org/conference-proceedings-of-spie on 6/5/2018 Terms of Use: https://www.spiedigitallibrary.org/terms-of-use

Design of Al-free and Al-based InGaAs/GaAs Strained Quantum Well 980 nm Pump Lasers including thermal behaviour effects on E/O characteristics

S.Pellegrino,M.G.Re,C.Beoni,D.Reichenbach,F.Vidimari
Alcatel-Telettra Research Center
Via Trento 30, 20059 Vimercate (Mi), Italy

Abstract

A two-dimensional thermal simulator and a model to evaluate high power lasers characteristics have been developed.
With these models it was possible to optimize cavity length of InGaAs/GaAs (Multiple) Quantum Well 980 nm lasers realized both with Al-based and Al-free confining layers.A comprehensive experimental investigation of the influence of cavity length and temperature on the laser emission wavelength has been performed.This allows a fine trimming of the devices to match the Erbium doped fiber absorption bandwidth.

Introduction

High power InGaAs/GaAs 980 nm Lasers have become of great interest for application as pump sources in Erbium Doped Fiber Amplifiers (EDFA).These devices are based on InGaAs/GaAs Single and Double Quantum Well (SQW,DQW) strained active layers and AlGaAs Separate Confinement Heterostructure (SCH).To improve their performances for high reliability applications (such as undersea links) Al-free devices based on InGaAsP/InGaP SCH are currently under investigation.It has been demonstrated [1], that the introduction of Indium increases the resistance to dark-line defect (DLD) motion, being the key to dislocation pinning.
By deliberate introduction of defects by scribing near the active stripe, a different behaviour has been found from, on one hand, devices with GaAs QW and, on the other hand, Indium bearing alloys either in the strained InGaAs active or as constituent of the unstrained InGaAsP active and InGaP cladding of 800 nm emitting devices.The former rapidly degrades due to fast growth of DLD along (100) direction, while the later show a DLD growth velocity which is two orders of magnitude lower than the GaAs one.
One of the key points in designing these devices is the choice of cavity length [2], in order to minimize operating current in the range of 150-200 mW emission power.
Furthermore, the emission wavelength of these devices has been found to be strongly dependent on the cavity length [3], which is a well known feature of semiconductor lasers, that might allow the fine trimming of the lasers to match the relatively narrow (roughly 10 nm) absorption bandwidth of the Erbium doped fibers.

0-8194-1445-X/94/$6.00

Downloaded From: https://www.spiedigitallibrary.org/conference-proceedings-of-spie on 6/5/2018 Terms of Use: https://www.spiedigitallibrary.org/terms-of-use

Results and discussion

The choice of device length is usually done considering only its influence on threshold current density (Jth) and Slope efficiency (Se) without taking into account all the effects of the thermal behaviour of the devices, which are not negligible in the high power regime.For this purpose a 2-D Thermal Simulator was developed exploiting Finite Differences Equations, suitable to evaluate temperature distribution for arbitrary structures and materials.The structure is assumed to be symmetrical, thus allowing a reduction in the calculation time, and is divided in regions of given thermal conductivity.For every block a physical area and the number of discretization points are defined; the discretization cell is a five points star which can be completely asymmetrical both in the discretization step and in the thermal conductivity [4].In the frame of such general formulation the adiabatic boundaries of an area are simply defined by imposing zero conductivty to the confining regions.
Finally the discretized equations are solved calling the D03UAF NAG routine; usually the convergence is fast and requests few minutes of VAX 8600 computing time.
A typical result which could be achieved for a Ridge Waveguide (RW) Laser structure is shown in figure 1.

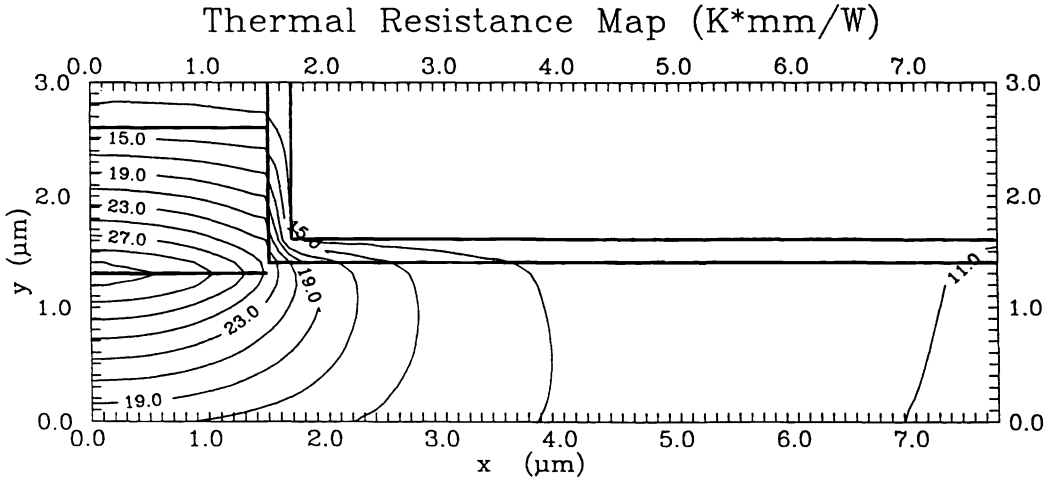

Figure 1: Thermal resistance map for a Al-based, junction-up mounted RW device with a 3 micrometrs wide ridge, planarized with a 5 micrometers thick gold heat spreader.

Downloaded From: https://www.spiedigitallibrary.org/conference-proceedings-of-spie on 6/5/2018 Terms of Use: https://www.spiedigitallibrary.org/terms-of-use

A wide range of technological options have been simulated, as an example in figure 2 is depicted the effect of the thickness of a gold heat spreader on the thermal resistance (Rth) for p-side-up mounted RW devices with different ridge widths.

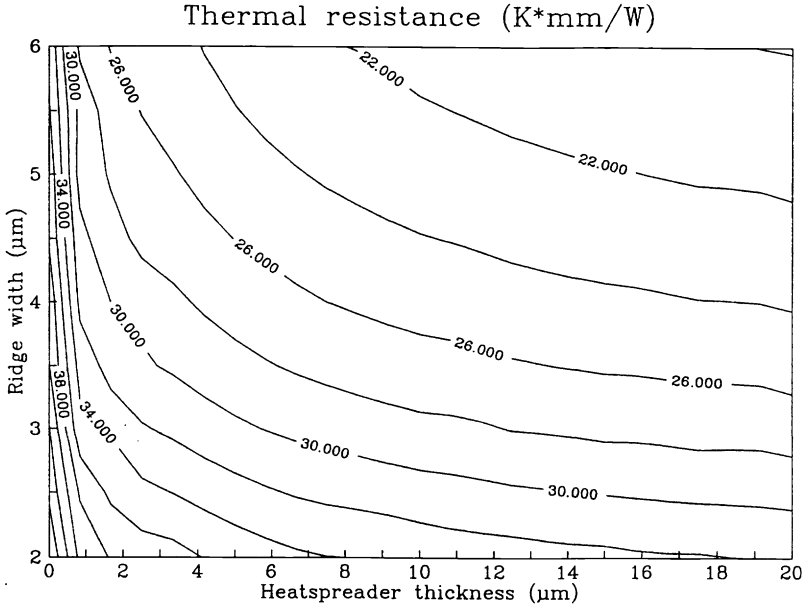

Figure 2: Thermal resistance dependence on RW width and heat spreader thickness; the thermal resistance value is averaged over the active layer lateral dimension.

In these two mentioned figures the thermal resistance values are normalized to 1 millimeter long devices, as Rth scales with 1/L.
In order to complete the description of laser characteristics, threshold and Slope efficiency on several SQW and DQW structures have been analyzed, both with Al.5GaAs and InGaP cladding layers.The waveguide structure comprises either Al.2GaAs and GaAs spacer, or InGaAsP (λgap=780-720 nm) and GaAs spacer for Al-based and Al-free structures, respectively.
Transmission Electron Microscopy investigation has been performed to extract precisely the waveguide dimensions which allow a detailed evaluation of gain characteristics.
The gain curves are well fitted by a logarithmic dependence like:

$$g_m=\Gamma G_0 \ln(J/J_{tr}) \qquad [1]$$

Transparency current values and modal differential gain coefficients are summarized in table 1.

Downloaded From: https://www.spiedigitallibrary.org/conference-proceedings-of-spie on 6/5/2018 Terms of Use: https://www.spiedigitallibrary.org/terms-of-use

	Jtr [A/cm2]	Γdg/dJ [cm/A]
SQW Al-based	74.0	0.31
DQW Al-based	125.4	0.30
SQW Al-free	110.3	0.28
DQW Al-free	185.7	0.25

Table 1: Transparency current density and differential gain coefficients used in the calculation.

Internal quantum efficiency higher than 90% are routinely measured for all structures.In the case of Al-based structures very low absorption coefficients, below 5 cm-1 are observed, while for InGaAsP/InGaP guides the values are somewhat spreaded, ranging from 4 to 8 cm-1.
Using the measured material parameters and the simulated thermal distribution we can evaluate the dependence of the threshold current (Ith), Slope efficiency, series resistance and thermal resistance versus the cavity length.
Moreover, assuming an exponential variation with temperature:

$$\eta_e = \eta_0 \exp(-T/T_1) \qquad [2]$$

we can get the output power from the front facet versus forward current (If) at different cavity lengths.
It is theoretically predicted, and experimentally demonstraded that the internal quantum efficiency has a strong variation with cavity length and operating temperature [5].It is clear then that the high power operation regime, leading to an increase of junction temperature, results in a reduction of internal efficiency which directly reflects in a decrement of the measured Slope efficiency.
This effect is expected to be more pronounced in the case of SQW respect to the MQW ones especially at higher temperatures.
Using the characteristic temperatures T0 and T1 as derived in figure 3, from our SQW devices (T0=130 K and T1=1400 K for a SCH Al-based SQW laser with AR/HR facet coatings) we can obtain a plot like the one shown in figure 4.

Downloaded From: https://www.spiedigitallibrary.org/conference-proceedings-of-spie on 6/5/2018 Terms of Use: https://www.spiedigitallibrary.org/terms-of-use

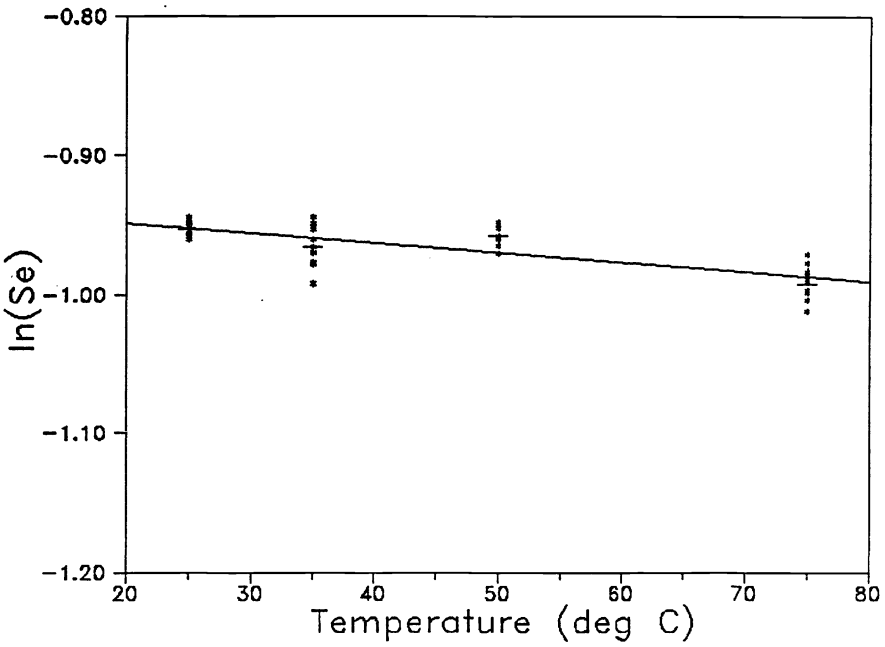

Figure 3: Slope efficiency versus temperature for an Al-based SQW laser structure; T1 parameter is 1400 K.

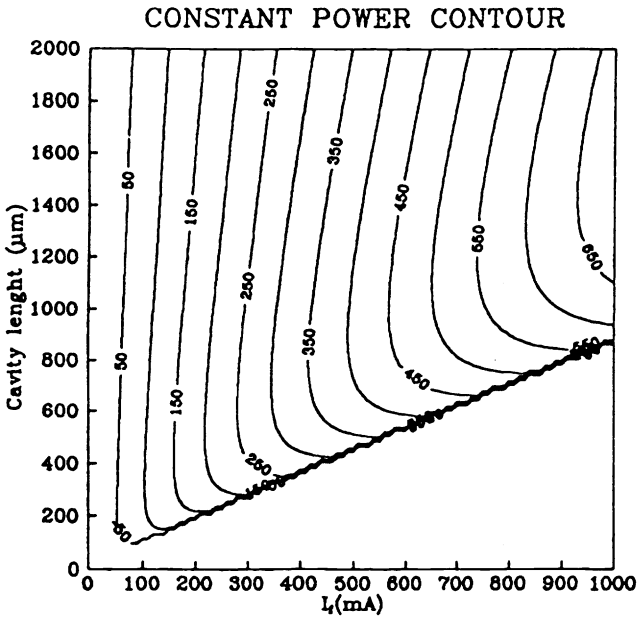

Figure 4: Constant power level curves dependence on laser cavity length and driving current.

Downloaded From: https://www.spiedigitallibrary.org/conference-proceedings-of-spie on 6/5/2018 Terms of Use: https://www.spiedigitallibrary.org/terms-of-use

The curves show constant emission power level, and the area below the straigth line at the bottom represents the turning-off conditions due to thermal runaway.
As it can be seen, for an output power of 200 mW the minimum operating current is around 200 mA, which corresponds to an optimum device length ranging between 500 and 600 micrometers.
Obviously the optimum cavity length is strongly affected by both characteristic temperature values, so a stronger Se dependence on temperature, as reported for example in reference [6], with a T1 value in the range of 130 K, results in a power versus driving current behaviour as shown in figure 5.

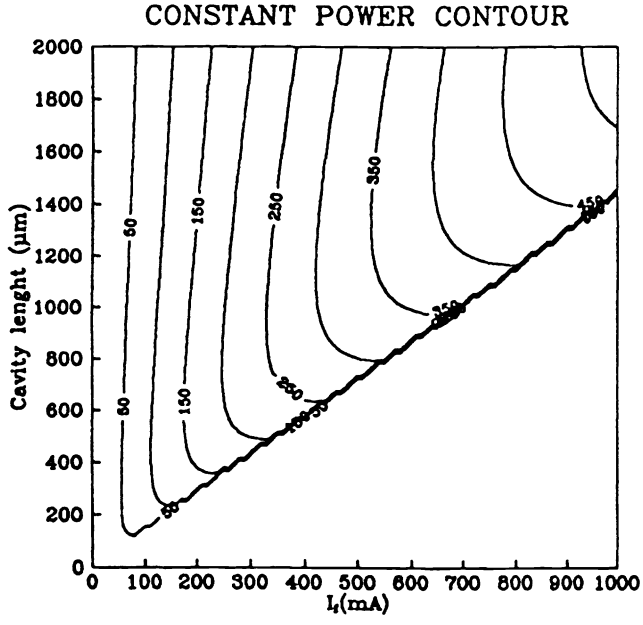

Figure 5: Constant power level curves respect to laser cavity length and driving current, in case of T1=130 K as derived from reference [6].

Here we can notice, for the same output power of 200 mW, that the optimum length raises to about 800 micrometers, with an operating current greater than 250 mA.Furthermore, the devices are optimized in a narrow power level range which imposes constrictions to their use.
In the case of high T1, as shown in figure 4, we can notice that the structures are optimized within 10% of the minimum operating current in a wide device length, up to operating power higher than 300 mW. This relatively large insensitivity to device length, for optimized structures, allows a wide tuning of the emission wavelength.In figure 6 is shown the dependence of the emission wavelength at threshold, which corresponds roughly to 10 nanometers span, in a device length region where its dependence is not yet extremely sharp [3].

Downloaded From: https://www.spiedigitallibrary.org/conference-proceedings-of-spie on 6/5/2018 Terms of Use: https://www.spiedigitallibrary.org/terms-of-use

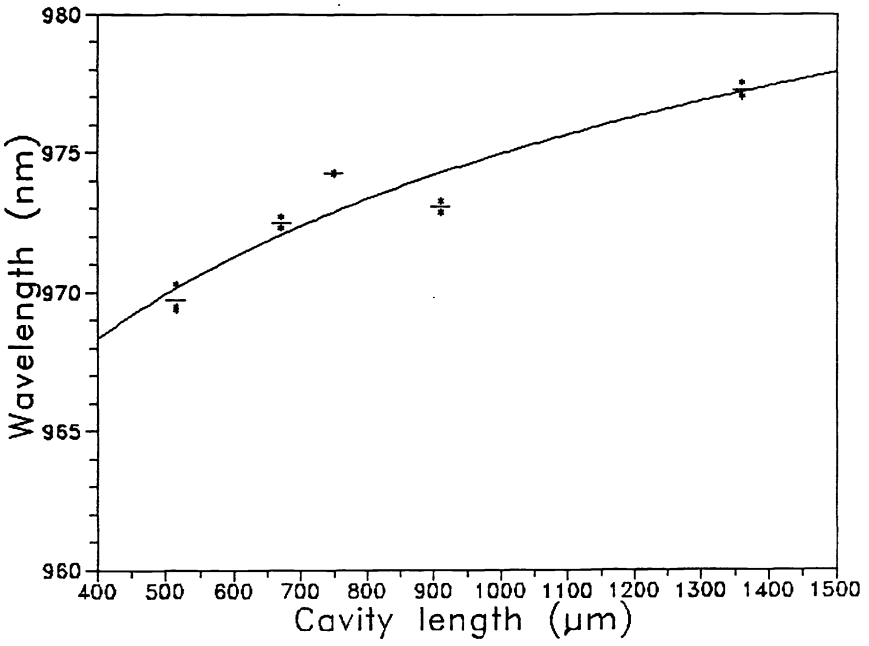

Figure 6: Emission wavelength dependence on cavity length for an Al-based SQW laser structure.

To fully account for the thermal effects in the high power regime it has to be taken into account that, above threshold the wavelength is tuned mainly by thermal effects, since the tuning slope is positive, as shown in figure 7.

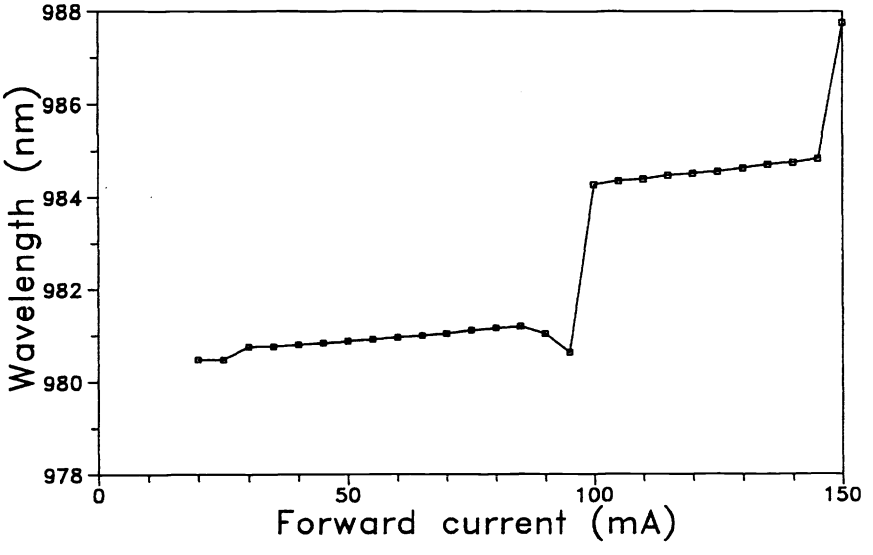

Figure 7: Lasing wavelength dependence on driving current for a 600 micrometers long RW Al-based SQW laser structure.

Downloaded From: https://www.spiedigitallibrary.org/conference-proceedings-of-spie on 6/5/2018 Terms of Use: https://www.spiedigitallibrary.org/terms-of-use

Finally, in addition to thermal effects, the other major limiting factor to high power operation is the Catastrophic Optical Damage (COD) of facet mirrors.Typical instantaneous COD power for Al-based devices is around 400 mW, which corresponds to roughly 100 mW/μm active, and then devices corresponding to figure 5 would be limited by thermal effects at high power.On the contrary, in case of our devices the COD limit should be reached just before the onset of thermal runaway.This behaviour is demonstrated on actual RW lasers 900 micrometers long and 4 micrometers wide, as shown in figure 8.

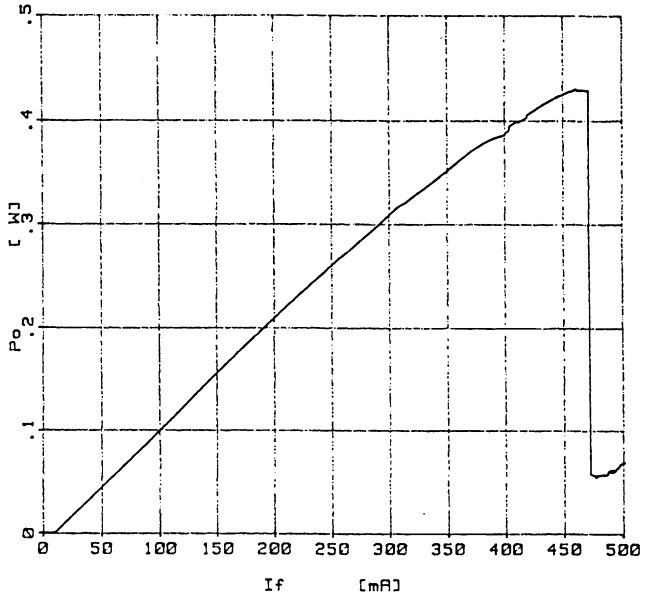

Figure 8: Power-current characteristc for a 900 micrometers long, 4 micrometers wide RW Al-based DQW.

Conclusions

A phenomenological model to evaluate the characteristics of lasers driven in the high power regime has been developed, accounting for the measured thermal behaviour on actual SQW and DQW, Al-based and Al-free devices emitting at 980 nm.The model should allow a precise determination of the device cavity length, in order to minimize the operating current and to fine trim the laser emission wavelength.The relative weight of the various thermal effects has been clarified experimentally and the optimized high power operation regime has been demonstrated.

Downloaded From: https://www.spiedigitallibrary.org/conference-proceedings-of-spie on 6/5/2018 Terms of Use: https://www.spiedigitallibrary.org/terms-of-use

Acknowledgements

The authors are indebt to Prof. I.Montrosset, Dr. M.Goano and Mr. E.Torasso from Politecnico di Torino for their valuable suggestions, and all the Alcatel-Telettra Laser Laboratory staff for their help during the work.

References

[1] S.L.Yellen,A.H.Shepard,C.M.Harding,J.A.Baumann,R.G.Waters, D.Z.Garbuzov,V.Pjataev,V.Kochergin, and P.S.Zory, "Dark-Line-Resistant, Aluminum-Free Diode Laser at 800 nm," IEEE Photon.Technol.Lett. 4 (1992) p.1328

[2] S.Oshiba, and Y.Tamura, "Recent progress in High Power GaInAsP Lasers," J.of Lightwave Technol. 8 (1990) p.1350

[3] T.R.Chen,Y.H.Zhuang,L.E.Eng, and A.Yariv, "Cavity length dependence of the wavelength of strained-layer InGaAs/GaAs lasers," Appl.Phys.Lett. 57 (1990) p.2402

[4] R.E.Bank, D.J.Rose, and W.Fichtner,"Numerical Methods for Semiconductor Device Simulation," IEEE Trans. Electron Devices, vol. ED-30, p.1031

[5] P.R.Claisse, and G.W.Taylor, "Internal Quantum Efficiency of Laser Diodes," Electron.Lett. 28 (1992) p.1991

[6] J.P.van der Ziel, and N.Chand,"High Temperature Operation (to 180°C) of 980 nm Strained Single Quantum Well In0.2GaAs/GaAs Lasers," App.Phys.Lett. 58 (1991) p.1437.

Downloaded From: https://www.spiedigitallibrary.org/conference-proceedings-of-spie on 6/5/2018 Terms of Use: https://www.spiedigitallibrary.org/terms-of-use